

**Error Analysis of Adsorption Isotherm Models for Sulfamethazine onto
Multi walled carbon nanotubes**

ABSTRACT

In the present study, Multi walled carbon nanotubes (MWCNTs) was used for the adsorption of Sulfamethazine (SMZ) antibiotics. The adsorbent was characterized by scanning electron microscopy, surface area (BET) and transmission electron microscopy. Batch experiments were carried out by varying the parameters like contact time, adsorbent dosage and initial Sulfamethazine concentration at fixed pH and temperature. The equilibrium data were tested with Langmuir, Freundlich, Tempkin, Dubinin–Radushkevich (D–R), Redlich-Peterson (R-P), Sips, Toth and Khan isotherm models at five Error Analysis EABS, X^2 , ARE, RMSE and SD and it was found that the Langmuir and Toth isotherms best fitted the adsorption of SMZ with highest value of R² and lowest overall experimental error. Also according to the results, a maximum removal efficiency of 99.1% was obtained at pH of 7 and the contact time of 60 min; initial SMZ concentration 20 mg/L and adsorbent dose 0.8 g/L.

Keywords: Batch adsorption; MWCNTs; Sulfamethazine; Isotherm.

1. INTRODUCTION

Due to the rapid population growth, water pollution, and increasing demand for clean water, advanced wastewater treatment is becoming an international focus for the rational use of scarce water resources and as a means of safeguarding aquatic environments from the harm caused by wastewater disposal (1-3). Reclamation and reuse of treated wastewater have become important topics in the sustainable management of water because high-quality water resources are becoming increasingly limited (4, 5).

As a result of soaring usage of antibiotics in the past decades, the significant residues of antibiotics in the aquatic environment have aroused great public concern, because of such bio-accumulative compounds might trigger antibiotic resistant gene upon long-term yet trace level of exposure (6, 7). Among various classifications of antibiotics, sulfonamide has been extensively used in both medication and cattle farming (8). Sulfamethazine (SMZ), which belongs to the sulfonamide group of antibiotics, is commonly used in veterinary medicine to control diseases and in livestock feeds for cattle and swine (9, 10). The SMZ residuals discharged from agricultural waste and municipal sewage tend to intrude into surface and ground water, that eventually result in deterioration of eco-system as well as public health (11, 12).

In the process of antibiotics removal from water, many technical methods, such as photodegradation, technical oxidation, biodegradation, and adsorption have been developed (13, 14). Considering the composition of wastewater is usually very complex and the concentration of antibiotic residues is as low as at ppm to ppb level, the efficiency of treatment methods remained great challenges (15, 16). Among these methods, adsorption has been proved to be an effective technique for its easy operation, high efficiency and inexpensive nature (17, 18). It is well documented that adsorption is a process whereby a contaminant adheres to the surface of an adsorbent, due to hydrophobic interaction, electrostatic interactions, π - π electron-donor–acceptor interactions and hydrogen bonds between the adsorbate and the adsorbent (19, 20).

Remediation of antibiotic-contaminated water has been achieved by sorption processes using various sorbents, including natural sorbents, clays, chitosan derivative, activated carbon, sorghum, Azolla, Lemna minor, carbon nanotubes, nano particles and etc (21-24). Various antibiotics sorption mechanisms including cation exchange, hydrophobic partitioning, and surface complexation reactions (H-bonding and other polar interactions) between the functionalities (amino, carboxyl and phenol) of the antibiotics molecules have been proposed (25, 26).

Due to a large surface area, small, hollow, and layered structures, carbon nanotubes (CNTs) have already been investigated as promising adsorbents for various organic pollutants and antibiotics (27, 28). Unlike many adsorbents, CNTs possess different features that contribute to the superior removal capacities; such as fibrous shape with high aspect ratio, large accessible external surface area, and well developed mesopores (29).

The Sulfamethazine ($C_{12}H_{14}N_4O_2S$) were used in the batch adsorption system to evaluate the potential of multi walled carbon nanotubes (MWCNTs) to remove this antibiotic from aqueous solution. The chemical structure of SMZ is presented in Fig. 1. Furthermore, the effects of SMZ initial concentration, adsorbent dosage and contact time on this process were investigated. Finally, the adsorption isotherms and kinetics were studied.

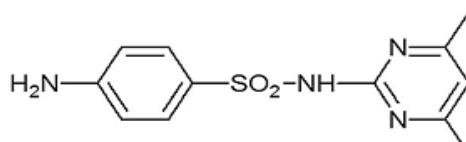


Fig. 1. The chemical structure of Sulfamethazine

2. MATERIALS AND METHODS

2.1 Chemicals and reagents

The multi-wall carbon nanotubes (MWCNTs) used in this study was of more than 98% purity and provided from Research Institute of Petroleum Industry (RIPI), Tehran, Iran). The size and morphology of MWCNTs were examined by scanning electron microscope (JEOL JSM 6500F) and transmission electron microscopy (TEM) (using a Philips XL30). SMZ antibiotics were purchased from the Sigma–Aldrich chemicals. All the other chemicals were obtained from Merck Co. (Germany) chemicals used for the study were of analytical grade.

2.2 Batch Adsorption Studies

Various experimental conditions which may be effective on the biosorption of SMZ by dried *A. filiculoides* including contact time (10-180 min), biosorbent dosage(0.1-1.5 g/L) and initial SMZ concentration(5-100 mg/L) were assessed in batch experiments. Initial SMZ solutions with different concentrations were prepared by diluting of SMZ stock solution (1000 mg/L) with distilled water. The pH was adjusted using either 0.1M HCL or 0.1M NaOH solution. The experiments in batch system were carried out in a 100 ml Erlenmeyer flask. In every experiment, a certain concentration of SMZ and specific dose of adsorbent spilled into the flask and completely mixed with shaker at 120 rpm for 90 min. the samples were consequently centrifuged at 3600 rpm for 10 min. All batch experiments were carried out in triplicate. The residual concentrations were measured using HPLC in λ_{max} of 267 nm (C18 column, methanol/water (50/50 v/v) mobile phase at a flow rate of 0.6 ml/min).

3.3 Experimental Analysis

The amount of adsorption at time t (Q_t , mg/g) was calculated by Eq (1) (30).

$$q_e = \frac{(C_0 - C_e)V}{M}$$

Where V (L) is the volume of the solution, C_0 and C_e (mg/L) are the concentrations of SMZ at initial and regular time t, respectively, and M (g) is the mass of dry adsorbent used.

3. RESULTS AND DISCUSSION

TEM and SEM images (Fig. 2 a and b) show the morphological structure of MWCNTs. Images clearly suggests the crystalline tubular structure of nanotubes. The inner diameter and the outer diameter of the MWCNTs are in the ranges of 5–10 nm and 40–50 nm, respectively. Fig. 2c and d shows the TEM and SEM images of SMZ adsorbed MWCNTs. Clusters of adsorbed SMZ over MWCNTs surface can be seen from the images. The BET surface area determined by N_2 adsorption is 702.5 m^2/g .

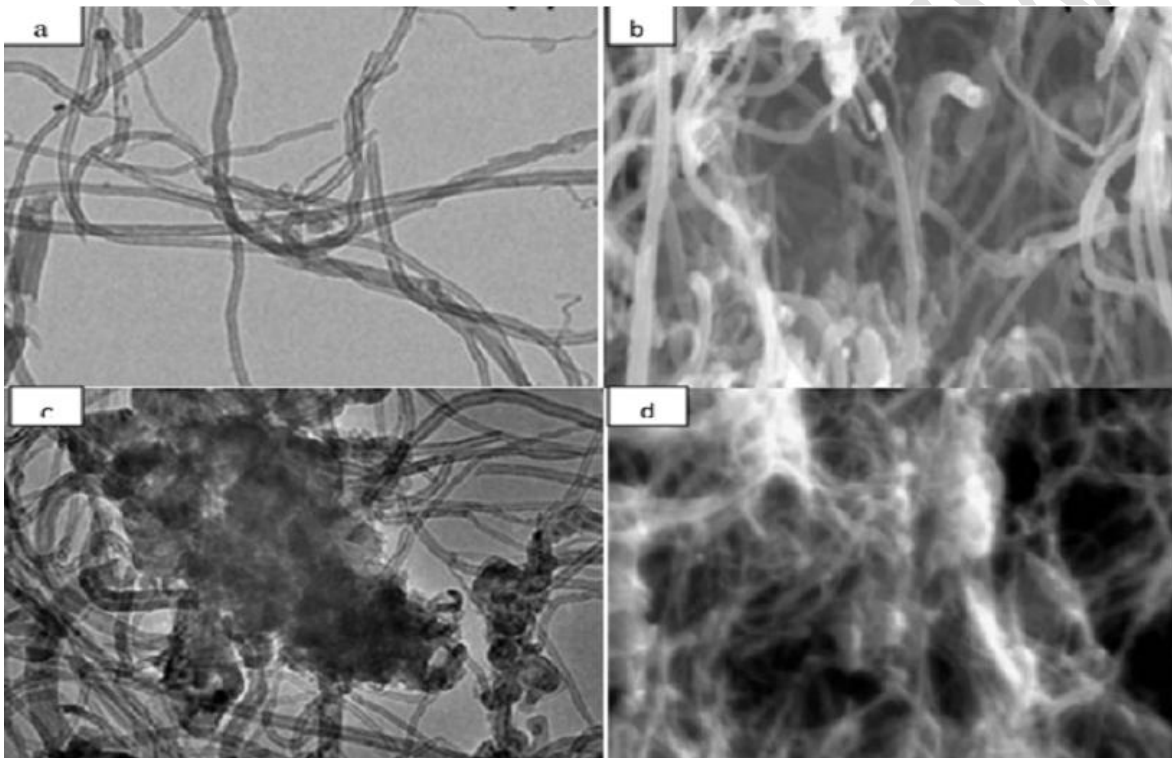


Fig. 2. TEM and SEM images of (a and b) MWCNTs and (c and d) SMZ adsorbed MWCNTs

The effect of MWCNTs dosage on the amount of SMZ adsorbed was studied by varying the amount of sorbent from 0.1 to 1.5 g/L whereas the SMZ concentration of 100 mg/L. All these studies were conducted at room temperature and at a constant agitation speed of 150 rpm. Fig 2 shows the effect of adsorbent dosage on the amount of SMZ adsorbed and it was observed that the amount of SMZ adsorbed decreased and the percentage SMZ removal was increased with increase in sorbent dosage of 0.1 g/L to 1.5 g/L. This was because of the increased total surface area and availability of more sites (31, 32). The SMZ uptake decreased from 344.1 mg/g to 60.25 mg/g. An increase in SMZ uptake was observed to decrease in adsorbent dosage. This may be due to the decrease in the total adsorption surface area available to SMZ from overlapping or aggregation of adsorption sites (33, 34). A similar result of the sorbent dose effect was also reported for the removal of antibiotics by nano carbon and nano particles (27, 28).

The influence of contact time (Fig 3A) was studied at room temperature (25 °C) while a sorbent dose of 0.8 g/L, a solution volume of 100 ml and an agitation speed of 150 rpm for a range of SMZ concentration. The rate of SMZ uptake was rapid at initial stage and equilibrium point has been reached within 60 min. This may be due to the fact that at the beginning of the sorption process all the reaction sites are vacant and hence the extent of removal is high (35, 36). After a rapid initial uptake, there was a transitional phase in which the rate of uptake was slow with uptake reaching almost a constant value. Consequently, the adsorption of SMZ was carried out in two distinct stages, a relatively rapid one followed by a slower one (39, 40). A similar result of the contact time effect was also reported for the adsorption of ciprofloxacin antibiotics from aqueous solution on red mud (33).

The effect of initial concentration on the adsorption of SMZ onto MWCNTs was deliberated by agitating 100 ml of SMZ solutions with concentrations of 20, 40, 60, 80, and 100 mg/L though the pH, shaking time, amount of sorbent, and temperature were fixed at 7, 60 min, 0.8 g/L, and 25 °C, respectively. It was observed that the amount of SMZ adsorbed increased with the increase of initial SMZ concentration (Fig 3B). Increasing the initial SMZ concentration increases the mass gradient between the solution and the adsorbent, and therefore, the rate at which SMZ molecules pass from the bulk solution to the particle surface and the amount of transfer at equilibrium (41, 42).

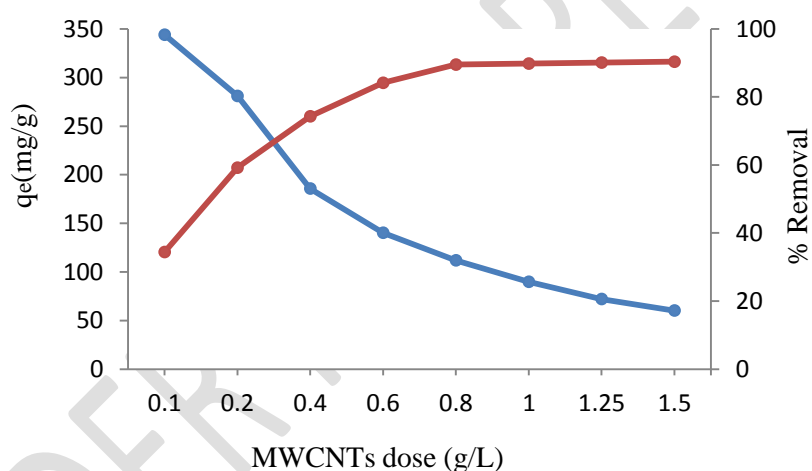


Fig. 3A. Effect of adsorbent dosage on SMZ adsorption ($C_0 = 100$ mg/L, time = 75 min, pH = 7, temp = $25 \pm 2^\circ\text{C}$ and mixing rate 150 rpm)

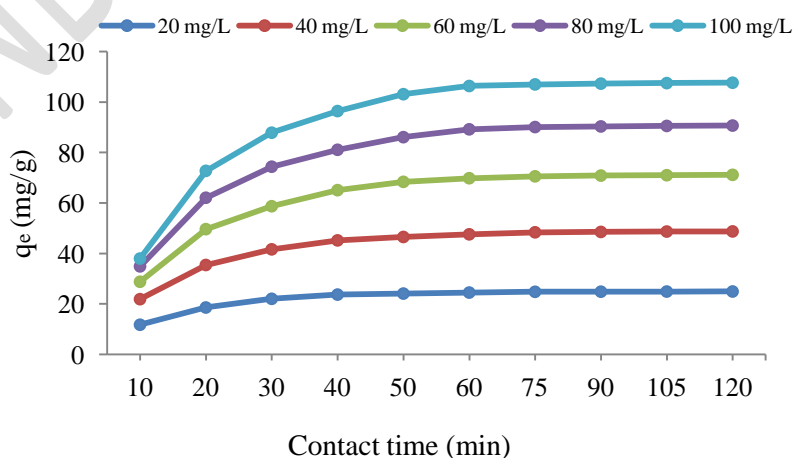


Fig. 3B. Effect of contact time and initial concentration on SMZ adsorption (pH = 7, Adsorbent dosage 0.8 g/L, mixing rate 150 rpm, temp = $25 \pm 2^\circ\text{C}$)

Adsorption isotherms

The application of adsorption isotherms is a prerequisite to understand the adsorbate-adsorbent interaction. The parameters described from the experimental data provide important information on the adsorption mechanisms and the surface properties. There are many equations for analyzing experimental adsorption equilibrium data. In this study, seven isotherm equations have been used, namely, Langmuir, Freundlich, Tempkin, Dubinin–Radushkevich (D–R), Redlich-Peterson, Sips, Toth and Khan models.

The Langmuir adsorption isotherm describes the surface as homogeneous assuming that all the adsorption sites have equal adsorbate affinity and that adsorption at one site does not affect adsorption at an adjacent site. The Langmuir equation is described in the following equation (43, 44):

$$\frac{C_e}{q_e} = \frac{1}{q_m K_L} + \frac{C_e}{q_m}$$

Where q_e is the amount of SMZ ion adsorbed at equilibrium (mg/g), C_e is the equilibrium concentration (mg/l), Q_m is the monolayer adsorption capacity (mg/g) and K_L is the constant related to the free adsorption energy (Langmuir constant, L/mg). A plot of C_e/q_e versus C_e gives a straight line of slope $1/q_m$ which corresponds to complete monolayer coverage (mg/g) and the intercept is $1/q_m \cdot K_L$.

The Freundlich isotherm describes the equilibrium on heterogeneous surfaces and does not assume monolayer capacity. The Freundlich equation is described by the following equations (45, 46):

$$Q_e = K_F C^{1/n}$$

The logarithmic form of the equation becomes:

$$\log q_e = \log K_F + \frac{1}{n} \log C_e$$

Where K_F is a constant indicative of the relative adsorption capacity of the adsorbent (mg/g) and the constant $1/n$ indicates the intensity of the adsorption. These constants were calculated from the slope and intercept of the Freundlich plots.

Tempkin isotherm considers the effects of the heat of adsorption that decreases linearly with coverage of the adsorbate and adsorbent interactions. Tempkin isotherm is represented by the following equation (47, 48):

$$Q_e = \frac{RT}{b} \ln A C_e \quad B=RT/b$$

$$Q_e = B \ln A + \frac{RT}{b} \ln C_e$$

Where A (L/g) and b are the Tempkin constants which can be determined from a plot of q_e versus $\ln C_e$.

Another equation used in the analysis of isotherms was proposed by Dubinin-Radushkevich (49):

$$Q_e = q_s \exp (-B\varepsilon^2)$$

Where q_s is the D–R constant and ε can be correlated as:

$$\varepsilon = RT \ln \left(1 + \frac{1}{C_e}\right)$$

The constant B gives the mean-free energy E of adsorption per molecule of the adsorbate when it is transferred to the surface of the solid from infinity in the solution and can be computed using the relationship (47):

$$E = \frac{1}{\sqrt{2B}}$$

Redlich-Peterson included the characteristics of both Langmuir and Freundlich isotherms into a single equation which incorporates three parameters into an empirical equation. It has a linear dependence on concentration in the numerator and an exponential function in the denominator to represent adsorption equilibrium over a wide range of concentrations. The R-P equation is widely used as a compromise between Langmuir and Freundlich systems (48):

$$Q_e = \frac{K_R C_e}{1 + a_R C_e^B}$$

Where K_R (l/g) and a_R (L/mg) are the Redlich–Peterson isotherm constants and B is the Redlich–Peterson model exponent. While B value tends to zero this isotherm approaches Freundlich isotherm and B value tends to unity this isotherm approaches Langmuir isotherm.

Sips model is combined form of Langmuir and Freundlich expression used for predicting the heterogenous adsorption system and overcoming the drawback associated with Freundlich isotherm model of continuing increase in the adsorbed amount with increase in concentration. Sips equation is similar to the Freundlich equation, but it has a finite limit when the concentration is sufficiently high (50).

$$Q_e = \frac{q_m K_s C_e^m}{1 + K_s C_e^m}$$

Where C_e is the equilibrium concentration of the adsorbate (mg/L), q_m and K are the Sips maximum adsorption capacity (mg/g) and Sips equilibrium constant (L/mg), respectively and m is the Sips model exponent.

The Toth isotherm is another empirical modification of the Langmuir equation with the aim of reducing the error between experimental data and predicted value of equilibrium data. This model is most useful in describing heterogeneous adsorption systems which satisfy both low and high end boundary of adsorbate concentration. The Toth isotherm model is expressed as follows (51):

$$\frac{q_e}{q_m} = \frac{C_e}{(K_T C_e^{nT})^{nT}}$$

Where q_m (mg/g) is the maximum monolayer adsorption capacity predicted by Toth isotherm, K_T is the Toth isotherm constant and nT is the Toth isotherm exponent. nT is a scale of surface heterogeneity. If nT approaches unity, this suggests that the process occurs on a homogenous surface.

Khan have suggested a generalized isotherm for the pure solutions. The khan isotherm model can be expressed as (52):

$$Q_e = \frac{q_m b_k C_e}{(1 + b_k C_e)^{a_k}}$$

With b_k and a_k are the Khan model constant and the Khan model exponent respectively.

Error analysis

The experimental data of the best represented kinetics and adsorption isotherm models were determined by the coefficient of determination value i.e. R^2 . The predicted q_e (q_e , cal) values

were generated using the formulae of various kinetics or isotherm models. Both the data predicted as well as experimental were fitted into the equations of diverse error analysis functions and the results having smallest value indicate the least error. The equations of the five types of error analysis are as follows (37, 38):

$$\text{Sum of the absolute error (EABS): } \sum_{i=1}^n (q_{e \text{ exp}} - q_{e \text{ cal}})$$

$$\text{Chi-square test (X}^2\text{): } \sum_{i=1}^n \left(\frac{q_{e \text{ exp}} - q_{e \text{ cal}}}{q_{e \text{ exp}}} \right)^2$$

$$\text{Average relative error (ARE): } \sqrt{\sum_{i=1}^n \left(1 - \frac{q_{e \text{ cal}}}{q_{e \text{ exp}}} \right)^2} \times \frac{100}{n}$$

$$\text{Root Mean Square Error (RMSE) = } \sqrt{\frac{\sum (q_{e \text{ exp}} - q_{e \text{ cal}})^2}{n}}$$

$$\text{SD} = \sqrt{\left(\frac{1}{N - P} \right) \sum_{i=1}^N (q_{i, \text{observed}} - q_{i, \text{calc}})^2}$$

Where $q_{e, \text{ exp}}$ is experimental value of q_e , $q_{e, \text{ cal}}$ is the predicted value of q_e by models, n indicates the number of data points in the experimental run.

The results of isotherm modeling data for are summarized in tables 1. The value of the R^2 of all the isotherm parameters was compared and found that the Langmuir model has the highest value of R^2 . Error function of all the parameters was compared and found that Langmuir model has lowest overall experimental error. Thus, it can be concluded from the foregone discussion that Langmuir model best represents the experimental data and is best suited model for the present work. The Langmuir model indicated the homogenous distribution of adsorption sites on the adsorption surface and this means a single layer of the SMZ molecules was formed on the surface. The R_L value comes between 0 and 1, indicated that adsorption process is favorable. The worst fitted model was D-R, which indicates the unsuitability to describe the adsorption characteristics.

Table 1: Results of isotherm parameters for the adsorption of SMZ onto MWCNTs

Langmuir		D-R		Freundlich		Tempkin	
q_m	109.4	q_m	54.72	K_F	8.921	A	0.472
K_L	0.384	E	0.582	n	2.346	B	35.46
R^2	0.997	R^2	0.912	R^2	0.825	R^2	0.841
ARE	1.85	ARE	9.125	ARE	11.35	ARE	17.25
RMSE	2.14	RMSE	11.66	RMSE	19.24	RMSE	14.66
X^2	0.79	X^2	3.641	X^2	6.142	X^2	7.451
SD	3.66	SD	7.254	SD	9.456	SD	11.95
EABS	4.12	EABS	8.926	EABS	14.61	EABS	17.24
R-P		Sips		Toth		Khan	
K_R	9.124	q_m	52.37	q_m	89.41	q_m	71.66
a_R	1.246	K_s	0.892	K_T	0.384	b_k	1449.2
q_m	64.12	m	0.241	nT	0.474	a_k	0.841
R^2	0.894	R^2	0.839	R^2	0.963	R^2	0.866
ARE	9.253	ARE	11.95	ARE	7.254	ARE	9.462
RMSE	8.461	RMSE	14.84	RMSE	6.985	RMSE	11.68
X^2	2.147	X^2	6.941	X^2	1.125	X^2	6.945
SD	5.941	SD	8.459	SD	8.452	SD	7.149
EABS	10.34	EABS	17.44	EABS	9.141	EABS	16.25

4. CONCLUSION

The effectiveness of MWCNTs in sorption of SMZ antibiotics from aqueous solution was explored and compared. The SMZ uptake rate was rapid and attains equilibrium within 60 min at fixed temperature 25 °C. Among all isotherm data obtained, the Langmuir model yields a better fit than other models. The maximum adsorption capacity determined by Langmuir at optimum condition was 109.4 mg/g. Error function provides the best parameters for the Langmuir isotherm equation for this system.

CONSENT

It is not applicable.

ETHICAL APPROVAL

It is not applicable.

COMPETING INTERESTS

Authors have declared that no competing interests exist.

REFERENCES

1. Choi KJ, Kim SG, Kim SH. Removal of antibiotics by coagulation and granular activated carbon filtration. *J. Hazard. Mater.* 2008; 151; 38–43.
2. Chena H, Bin Gaoa B, Lib H. Removal of sulfamethoxazole and ciprofloxacin from aqueous solutions by graphene oxide. *Journal of Hazardous Materials.* 2015; 283; 201-07.
3. Zhang W, He G, Gao P, Chen G: Development and characterization of composite nanofiltration membranes and their application in concentration of antibiotics. *Sep Purif Technol* 2003, 30:27–35.
4. Su YF, Wang GB, Kuo DTF, Chang ML. Photoelectrocatalytic degradation of the antibiotic sulfamethoxazole using TiO₂/Ti photoanode. *Applied Catalysis B: Environmental.* 2016; 186; 184-92.
5. Balarak D, Mostafapour FK, Joghataei A. Experimental and Kinetic Studies on Penicillin G Adsorption by Lemna minor. *British Journal of Pharmaceutical Research.* 2016; 9(5): 1-10.
6. Rostamian R, Behnejad H. A comparative adsorption study of sulfamethoxazole onto graphene and graphene oxide nanosheets through equilibrium, kinetic and thermodynamic modeling. *Process Safety and Environmental Protection.* 2016; 102; 20-29.
7. Hu L, Flanders PM, Miller PL, Strathmann TJ. Oxidation of sulfamethoxazole and related antimicrobial agents by TiO₂ photocatalysis *Water Research* 2007; 41(12); 2612-26.
8. Yu F, Li Y, Han S, Jie Ma J. Adsorptive removal of antibiotics from aqueous solution using carbon materials. *Chemosphere.* 2016; 153; 365–85.
9. Garoma T, Umamaheshwar SH, Mumper A. Removal of sulfadiazine, sulfamethizole, sulfamethoxazole, and sulfathiazole from aqueous solution by ozonation. *Chemosphere.* 2010; 79; 814–20.
10. Rostamian R, Behnejad H. A comparative adsorption study of sulfamethoxazole onto graphene and graphene oxide nanosheets through equilibrium, kinetic and thermodynamic modeling. *Process Safety and Environmental Protection.* 2016; 102; 20-29.
11. Balarak, D, Joghataei A, Mostafapour FK. Ciprofloxacin Antibiotics Removal from Effluent Using Heat-acid Activated Red Mud. *British J Pharm Res.* 2017; 20(5); 1-11.
12. Balarak D, Mostafapour FK, Azarpira H. kinetic and Equilibrium Studies of Sorption of Metronidazole Using Graphene Oxide. *British J Pharm Res.* 2017; 19 (4); 1-10.
13. Ji L, Chen W, Duan L and Zhu D. Mechanisms for strong adsorption of tetracycline to carbon nanotubes: A comparative study using activated carbon and graphite as adsorbents. *Environ Sci Technol.* 2009, 43 (7), 2322–27.
14. Balarak D, Azarpira H, Mostafapour FK. Study of the Adsorption Mechanisms of Cephalexin on to *Azolla Filiculoides*. *Der Pharma Chemica.* 2016, 8(10):114-121.

15. Gulkowsk A, Leung HW, So MK, Taniyasu S, Yamashita N. Removal of antibiotics from wastewater by sewage treatment facilities in Hong Kong and Shenzhen, China. *Water Research*. 2008; 42:395-403.
16. Zhang W, He G, Gao P, Chen G: Development and characterization of composite nanofiltration membranes and their application in concentration of antibiotics. *Sep Purif Technol*. 2003, 30:27–35.
17. Zhu XD, Wang YJ, Sun RJ, Zhou DM. Photocatalytic degradation of tetracycline in aqueous solution by nanosized TiO₂. *Chemosphere*. 2013; 92; 925–32.
18. Balarak D, Azarpira H. Rice husk as a Biosorbent for Antibiotic Metronidazole Removal: Isotherm Studies and Model validation. *International Journal of ChemTech Research*. 2016; 9(7); 566-573.
19. Aksu Z, Tunc O. Application of biosorption for Penicillin G removal: Comparison with activated carbon. *Process Biochemistry*. 2005;40(2):831-47.
20. Balarak D, Mostafapour FK, Joghataei A. Biosorption of amoxicillin from contaminated water onto palm bark biomass. *Int J Life Sci Pharma Res*. 2017; 7(1);9-16
21. Balarak D, Mostafapour FK. Batch Equilibrium, Kinetics and Thermodynamics Study of Sulfamethoxazole Antibiotics onto *Azolla filiculoides* as a Novel Biosorbent. *British J Pharm Res*. 2016; 13 (2); 1-10.
22. Braschi I, Blasioli S, Gigli L, Gessa CE, Alberti A, Martucci A. Removal of sulfonamide antibiotics from water: evidence of adsorption into an organophilic zeolite Y by its structural modifications. *Journal of Hazardous Materials*. 2010; 178:218–225.
23. Gobel A, Thomsen A, McArdell CS, Joss A, Giger W. Occurrence and sorption behavior of sulfonamides, macrolides, and trimethoprim in activated sludge treatment. *Environmental Science & Technology*. 2005; 39:3981–3989.
24. Huang M, Tian S, Chen D, Zhang W, Wu J, Chen L. Removal of Sulfamethazine antibiotics by aerobic sludge and an isolated *Achromobacter* sp S-3. *Journal of Environmental Sciences-China*. 2012; 24:1594–159.
25. Li B, Zhang T. Biodegradation and adsorption of antibiotics in the activated sludge process. *Environmental Science & Technology*. 2010; 44:3468–3473.
26. Perez S, Eichhorn P, Aga DS. 2005. Evaluating the biodegradability of Sulfamethazine, sulfamethoxazole, sulfathiazole, and trimethoprim at different stages of sewage treatment. *Environmental Toxicology and Chemistry* 24:1361–1367.
27. Balarak D, Mahdavi Y, Maleki A, Daraei H and Sadeghi S. Studies on the Removal of Amoxicillin by Single Walled Carbon Nanotubes. *British Journal of Pharmaceutical Research*. 2016;10(4): 1-9.
28. Balarak D, Mahdavi Y and Mostafapour FK. Application of Alumina-coated Carbon Nanotubes in Removal of Tetracycline from Aqueous Solution. *British Journal of Pharmaceutical Research*. 2016; 12(1): 1-11.
29. Ji L, Chen W, Duan L and Zhu D. Mechanisms for strong adsorption of tetracycline to carbon nanotubes: A comparative study using activated carbon and graphite as adsorbents. *Environ. Sci. Technol.*, 2009, 43 (7), 2322–27.
30. Zhang L, Song X, Liu X, Yang L, Pan F, Lv J. Studies on the removal of tetracycline by multi-walled carbon nanotubes, *Chem. Eng. J*. 2011; 178; 26–33.
31. Gao J and Pedersen JA. Adsorption of Sulfonamide Antimicrobial Agents to Clay Minerals. *Environ. Sci. Technol*. 2005, 39(24). 9509-16.
32. Putra EK, Pranowoa, Sunarsob J, Indraswatia N, Ismadjia S. Performance of activated carbon and bentonite for adsorption of amoxicillin from wastewater: mechanisms, isotherms and kinetics. *Water Res*. 2009; 43, 2419-30.
33. Balarak D, Mostafapour FK, Joghataei A. Kinetics and mechanism of red mud in adsorption of ciprofloxacin in aqueous solution. *Biosci Biotechnol Res commun*. 2017; 10(1);241-248.
34. Balarak D, Mostafapour FK, Azarpira H. Langmuir, Freundlich, Temkin and Dubinin-radushkevich Isotherms Studies of Equilibrium Sorption of Ampicillin onto Montmorillonite Nanoparticles. *British J Pharm Res*. 2016; 20 (2); 1-10.

35. Dutta M, Dutta NN, Bhattachary KG. Aqueous phase adsorption of certain beta-lactam antibiotics onto polymeric resins and activated carbon. *Separation and Purification Technology*.1999;16(3);213-24.
36. Peterson JW, Petrasky LJ, Seymour MD, Burkharta RS, Schuiling AB. Adsorption and breakdown of penicillin antibiotic in the presence of titanium oxide nanoparticles in water. *Chemosphere*. 2012;87(8); 911-7.
37. Chen WR, Huang CH. Adsorption and transformation of tetracycline antibiotics with aluminum oxide. *Chemosphere*. 2010; 79, 779-85.
38. Xu L, Pan J, Dai J, Li X, Hang H, Cao Z, Yan Y. Preparation of thermal-responsive magnetic molecularly imprinted polymers for selective removal of antibiotics from aqueous solution. *Journal of Hazardous Materials*. 2012; 233-234;48-56.
39. Rivera-Jiménez SM, Hernández-MaldonadoAJ. Nickel(II) grafted MCM-41: A novel sorbent for the removal of Naproxen from water. *Microporous and Mesoporous Materials*. 2008;116(1-3); 246-52.
40. Adrianoa WS, Veredasb V, Santanab CC, Gonçalves LRB. Adsorption of amoxicillin on chitosan beads: Kinetics, equilibrium and validation of finite bath models. *Biochemical Engineering Journal*. 2005; 27(2) ;132-37.
41. Erşan M, Bağd E. Investigation of kinetic and thermodynamic characteristics of removal of tetracycline with sponge like, tannin based cryogels. *Colloids and Surfaces B: Biointerfaces*. 2013; 104;75-82.
42. Balarak D, Mostafapour FK, Akbari, H. Adsorption of Amoxicillin Antibiotic from Pharmaceutical Wastewater by Activated Carbon Prepared from *Azolla filiculoides*. *British J Pharm Res*. 2017; 18(3); 1-10.
43. Balarak D, Azarpira H. Photocatalytic degradation of sulfamethoxazole in water: investigation of the effect of operational parameters. *Inter J Chem Tech Res*. 2016; 9(12):731-8.
44. Balarak D, Mostafapour FK, Azarpira H. Adsorption Kinetics and Equilibrium of Ciprofloxacin from Aqueous Solutions Using *Corylusavellana* (Hazelnut) Activated Carbon. *British J Pharm Res*.2016; 13 (3); 1-10.
45. Balarak D, Mostafapour FK, Bazrafshan E, Saleh TA. Studies on the adsorption of amoxicillin on multi-wall carbon nanotubes. *Water Sci technol*. 2017; 75(7); 1599-1606
46. Balarak D, MostafapourFK. Batch Equilibrium, Kinetics and Thermodynamics Study of Sulfamethoxazole Antibiotics Onto *Azolla filiculoides* as a Novel Biosorbent. *British J Pharm Res*.2017;13(2); 1-11.
47. Balarak D, MostafapourFK, Khatibi AD. Nonlinear Isotherms and Kinetics and Application Error Functions for Adsorption of Tetracycline on *Lemna Minor* *British J Pharm Res*. 2018;23(2); 1-11.
48. Yu F, Li Y, Han S, Jie Ma J. Adsorptive removal of antibiotics from aqueous solution using carbon Materials. *Chemosphere*. 2016;153;365–385.
49. Aksu Z, Tunc O. Application of biosorption for Penicillin G removal: Comparison with activated carbon. *Process Biochem*. 2005;40(2):831-47.
50. Balarak D, Mostafapour FK, Joghtaei A. Thermodynamic Analysis for Adsorption of Amoxicillin onto Magnetic Carbon Nanotubes. *British J Pharm Res*.2017; 16 (6); 1-10.
51. Putra EK, Pranowoa R, Sunarsob J, Indraswatia N, Ismadjia S. Performance of activated carbon and bentonite for adsorption of amoxicillin from wastewater: mechanisms, isotherms and kinetics. *Water Res*. 2009; 43, 2419-2430.
52. Adrianoa WS, Veredasb V, Santanab CC, Gonçalves LRB. Adsorption of amoxicillin on chitosan beads: Kinetics, equilibrium and validation of finite bath models. *Biochem Eng J*. 2005; 27(2); 132-37.